Response of Airline Pilots to Variations in Flight Simulator Motion Algorithms

Lloyd D. Reid* and Meyer A. Nahon†
University of Toronto Institute for Aerospace Studies, Toronto, Ontario, Canada

The use of physical motion in flight simulation is still a much debated topic. This paper investigates the more narrow issue of its application in commercial jet transport simulators. We have attempted to quantify the perceptions of airline pilots about the quality of motion possible when a number of different motion-drive algorithms are tested on a simulator employing a state-of-the-art six-degrees-of-freedom motion-base. Four broad categories of algorithms were tested: classical washout, optimal control, coordinated adaptive, and no-motion. It was found that although there was little impact of algorithm type on performance and control activity, there was a definite effect on how the pilots perceived the simulation environment. Based on these findings, it appears that the coordinated adaptive algorithm is generally preferred by the pilots over the other algorithms tested. There was almost unanimous dislike of the no-motion case.

Introduction

THE present study was prompted by the need to install a motion-drive algorithm on the recently commissioned University of Toronto Institute for Aerospace Studies (UTIAS) Flight Research Simulator, shown in Fig. 1. It was felt that perhaps one of the more recent developments, such as adaptive or optimal control algorithms, would be best suited to such a research facility.

A review of recent reports covering the design and evaluation of motion-drive algorithms was carried out, with the awareness that the present system is a six-degrees-of-freedom synergistic motion-base with hydrostatic bearings. As might be expected, a perfect match between our needs and the reported material was not found, although some very helpful information was located. For example, the work implemented in Ref. 1 was carried out on a simulator employing hydrostatic bearings but was restricted to three degrees-of-freedom. Reference 2 utilized six degrees-of-freedom but involved the simulation of combat aircraft, as did Ref. 3 (but with five degrees-of-freedom). The studies reported in Refs. 4 and 5 employed the simulation of a B737 and came closest to satisfying our requirements (although only five degrees-of-freedom were active). In fact, the nonlinear-coordinated adaptive washout routine from these latter two references formed the basis for the adaptive washout algorithms studied in the present project. The work reported in Ref. 6 was found to be extremely helpful. It indicated that the adaptive washout was preferred by pilots over the classical fixed filter washout in a three-degrees-of-freedom helicopter simulation. A comparison between an optimal control and a classical washout is presented in Ref. 7, where no significant differences in pilot preference were found in a two-degrees-of-freedom simulation of a VTOL aircraft.

Following this review, it was decided to carry out a study to obtain pilot evaluations of the motion quality produced by classical washout, optimal control, and adaptive washout, using the full six degrees-of-freedom of our motion base. It was anticipated that the findings would also help to clarify the relative merits of the various alternatives for commercial jet transport training simulators.

Received June 1, 1987; revision received Aug. 27, 1987.

*Professor and Associate Director. Associate Fellow AIAA.
†Project Engineer.

Description of the UTIAS Flight Research Simulator

The motion base of the UTIAS Flight Research Simulator is a CAE Series 300 six-degrees-of-freedom synergistic unit incorporating hydrostatic bearings. Its performance characteristics are fully documented in Ref. 8, and a summary of its motion limits is contained in Table 1. Its signal-to-noise properties and dynamic response are equal to or better than most current commercial systems. A DC-8 cab is mounted on the motion base and the whole system is run at a 20 Hz update rate by a Perkin Elmer 3250 digital computer. Engine and aerodynamic sounds are generated by a digital system controlled by the computer. The other major components are outlined below. A detailed description is contained in Ref. 9.

Aircraft Equations

The simulated aircraft was a Boeing 747. The flight equations were based on Refs. 10–12. The aerodynamic forces and moments were obtained from Ref. 11 and stored in the form of lookup tables. The equations were solved using a second order Adams-Bashforth numerical integration scheme. A full set of ground handling equations was developed as well, along with a JT9D-3 engine model derived from Ref. 11.

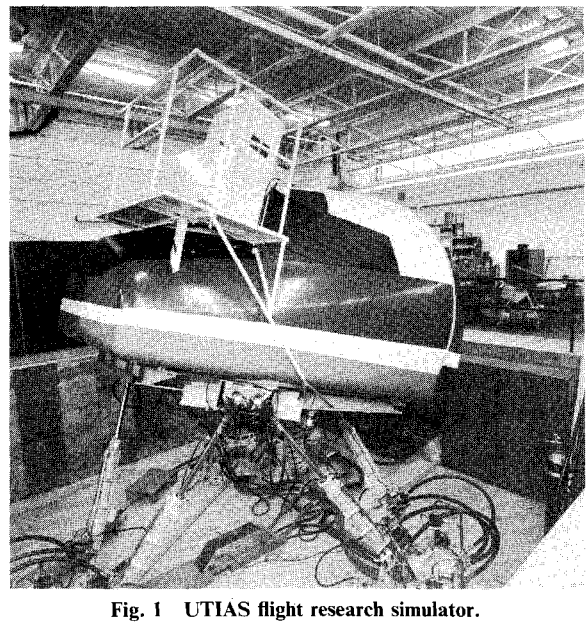

Fig. 1 UTIAS flight research simulator.

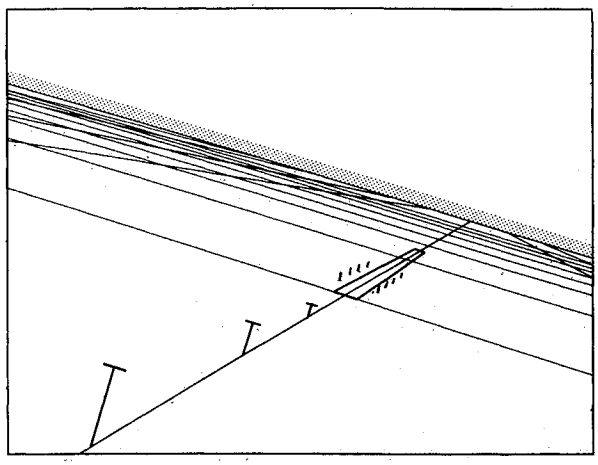

Fig. 2 Head-up display.

Navigation and Landing Aids

Navigation and landing aids were generated to represent an airport terminal area. The runway has an instrument landing system (ILS) with a 3 deg glideslope. This was sufficient to allow the pilots to complete the flying tasks associated with this study.

Visual Display System

The forward out-the-window CRT display is viewed through a collimating optical unit employing a beam splitter and a mirror (from a VITAL II system). The field of view is 40 deg horizontally and 30 deg vertically. The monochromatic image (yellow) is produced by a vector generator driven by the Perkin Elmer 3250 digital computer, and consists of straight line segments on a dark background. This system is used to produce a head-up display representing the outside world in perspective, as shown in Fig. 2. The display is updated at 20 Hz.

The ground plane is represented by a grid of squares, and horizon glow is also included. A set of three T-bars along the approach to the runway is provided as a visual aid to landing. When the aircraft is on the localizer and glideslope, all the T-bars are aligned and the pilot should attempt to fly through their cross-piece intersection points. A set of pole indicators beside the runway acts as a visual aid during the flare portion of the landing maneuver. This display was quite natural to use and the pilots had no difficulty performing their flying tasks while looking out the window.

Turbulence

Turbulence effects are included in the simulation through the wind velocity at the aircraft's center of mass and the wind gradient in the spanwise direction. The effect of turbulence on the horizontal tail is accounted for by incrementing its angle of attack by a time delayed version of the increment in the wing's angle of attack due to turbulence (i.e., the frozen flow assumption). In all, three components of turbulence and two of turbulence gradient are generated as independent non-Gaussian processes. The technique employed is the one described in Refs. 13–15. The resulting patchy turbulence was fairly realistic. The intensity of the turbulence was reduced smoothly from moderate to zero near the runway so as not to disturb the aircraft during the final phase of the landing approach.

Buffet and Runway Roughness

The buffet vibration is intended to be representative of the buffet felt in an aircraft as a result of the flaps and landing gear being exposed to the slipstream. The runway roughness is intended to indicate to the pilot that the wheels of the aircraft are making ground contact. Only very simple sinusoidal waveforms are employed and no attempt is made to duplicate actual motion time histories. The signals are fed directly to the motion base without passing through the washout filters and hence are unaffected by changes to the washout algorithms. The same motion increment is applied to all six actuators, thereby producing primarily a heave of acceleration.

Motion and Visual Cue Timing

The relative time between the various steps in the simulation process is important in determining the quality of the simulation as perceived by the pilot. In the present instance, the complete sequence of events corresponding to one iteration cycle takes place in 50 ms. The overall time delay sensed by the pilot depends on both the software and the hardware. The out-the-window visual display and the motion drive command signals are both generated by the Perkin Elmer 3250 computer. Based on computer generated measurements of execution times for the softwart and dynamic response measurements for the motion base using accelerometers and rate gyros, the following time delay estimates were obtained for two scenarios. Under normal operating conditions with smooth continuous inputs, the additional time delays between pilot input on the controls and a visual display or motion response, beyond that due to the aircraft equations of motion (allowing 25 ms of delay to represent an average value for the time delay in sampling the pilot's input, are: visual time delay, 14-24 ms; motion time delay, 0-50 ms. In the case where a discontinuous step input by the pilot is assumed to be the test signal, these time delays are increased:

Visual time delay	114-124 ms
Motion time delay	
Classical and optimal algorithms	60-110 ms
Adaptive algorithm	160-210 ms

It is felt that no significant time delay effects were experienced in the present study.

Motion-Base Drive Algorithms

Three types of motion-base drive algorithms were studied in the present project (in addition to a no-motion case):

1) Classical washout of the type currently employed in airline flight simulators[16-18]
2) Optimal control[19]
3) Coordinated adaptive.[5]

Our interest was in adapting them for use on the UTIAS Flight Research Simulator and in obtaining an unbiased assessment of the quality of the motion they produce. The details of the exact form of the resulting algorithms are presented in Refs. 20 and 21. A brief description outlining their key features is given in the following section.

Classical Washout

In the classical washout algorithm, fixed coefficient high-pass filters are used to prevent low frequency linear acceleration signals from reaching the motion-base. This is done because it is these low frequency signals that can cause the simulator motion system to exceed its physical displacement limits. The same process is used in the yaw degree-of-freedom, mainly to wash out the large yaw angles associated with steady turns. A process known as tilt-coordination is used to generate simulator low frequency pitch and roll angles in response to low frequency aircraft longitudinal and lateral specific force. This aligns the simulator pilot relative to the local gravity vector so that his vestibular system senses a resultant specific force with the same relative orientation as that sensed by the pilot in the aircraft. If done properly, this can be used to create the illusion of sustained longitudinal and lateral acceleration. To be successful, the simulator's angular tilt rates must go undetected by the pilot during this process. For this reason tilt rate limiting of 3 deg/s is employed in the present study. Another feature of the crossfeed from aircraft specific force to simulator tilt is that during a coordinated turn, the simulator bank angle (generated as the initial aircraft roll-rate begins) is washed out, returning the simulator to a level condition and thereby generating the

correct sensation of zero sustained lateral specific force during the turn. A combination of the low frequency crossfeed and high-pass filters applied to the aircraft pitch and roll rates tends to produce an unfiltered overall simulator response to uncoordinated aircraft pitch and roll. In the case of a jet transport simulation, because the actual aircraft pitch and roll displacements are relatively small, this causes no serious problem.

Optimal Controller

Like classical washout, the optimal controller algorithm uses fixed coefficient high-pass filters and low-pass crossfeed filters to restrict the motion of the flight simulator. Two significant differences, however, are the use of optimal control theory to select the form of the filters and the optimal controller's attempt to match the pilot's vestibular sensations in the aircraft and in the simulator. The latter requires the use of a linear mathematical model of the vestibular system. The filters are similar in function to those in the classical washout. However, it was found that rate limiting could not be used on the tilt-coordination crossfeed because this caused excessive bank angles in the simulator during coordinated turns. This results from the use of lateral acceleration in the crossfeed channel by the optimal controller. (Classical washout uses lateral specific force.)

Coordinated Adaptive Washout

This algorithm is somewhat similar in general structure to the classical washout. The significant difference is the use of an adaptive control scheme to continuously adjust the parameters in the filters in response to the current state of the simulator motion base. As the motion limits are approached the filters become more restrictive. This allows the use of fairly modest filtering during the rest of the time, thereby improving the overall quality of motion. It is found that care must be taken in selecting the system gains and in limiting the range of the adaptive parameters in order to avoid instabilities.

Table 1 Motion limits for the UTIAS flight research simulator[a]

Roll	Displacement	±20.8 deg
	Velocity	34.4 deg/s
	Acceleration	400 deg/s^2
Pitch	Displacement	+21.3 deg, −19.8 deg
	Velocity	34.4 deg/s
	Acceleration	400 deg/s^2
Yaw	Displacement	±23.7 deg
	Velocity	34.4 deg/s
	Acceleration	400 deg/s^2
Surge	Displacement	+0.61, −0.70 m
	Velocity	0.80 m/s
	Acceleration	10 m/s^2
Sway	Displacement	±0.59 m
	Velocity	0.80 m/s
	Acceleration	10 m/s^2
Heave	Displacement	+0.55, −0.49 m
	Velocity	0.80 m/s
	Acceleration	10 m/s^2

[a]Based on motion of or about the centroid of the upper frame.

Selecting Algorithm Parameters

In order to generate a range of motion-base drive algorithms for testing, three parameter sets were generated for each algorithm type. Complete details are contained in Refs. 9, 20 and 21. The tuning process involved choosing washout filter parameters which would yield a range of simulator motions, from the most active (while still remaining within the limits of the motion base of the UTIAS Flight Research Simulator) to the least active, for a given set of aircraft maneuvers.

The classical washout (CW) filters were tuned by modifying the filter characteristics. In all cases, a scale factor of 0.5 was applied to the motion variables coming from the flight equations. The most active version, CW1, was chosen to produce simulator motions close to the maximum actuator travel available, while responding to the three design maneuvers. The second set, CW2, had the same order filters as CW1 but was tuned to have a more restricted low frequency response. The third set, CW3, was chosen to be even more restrictive and had all its high-pass filters increased by one order.

In the case of the optimal controller (OC), the same scale factor of 0.5 was used at the input. The most active version, OC1, was created by adjusting the weights of its cost functional to achieve the same level of response as CW1 to the design maneuvers. The second set, OC2, was taken to be the same as OC1, except that it was altered to allow more simulator roll. The third set, OC3, was obtained by starting with OC1 and increasing the penalty in the cost functional associated with simulator motion, thereby creating a more restrictive filter.

The coordinated adaptive washout (AW) algorithms were tuned by starting with input scale factors of 1.0, 0.5 and 0.25 for AW1, AW2 and AW3, respectively. The fixed algorithm parameters for AW1 were then selected to give peak simulator motion similar to CW1 for the test maneuvers. The parameters for AW2 were selected to give peak responses similar to CW2. In addition, an attempt was made in going from AW1 to AW2 to reduce the false lateral specific force cue in roll maneuvers due to excessive simulator roll and its slow return to the neutral position. AW3, the most restrictive filter set of the three, was identical to AW2 except for the aforementioned scale factors.

Experimental Design

Because the purpose of this study was to assess the suitability of motion-base drive algorithms for use in jet transport flight simulators, it was decided to employ current airline pilots in the evaluation process. The primary assessment consisted of having the pilots fly a flight sequence in the UTIAS Flight Research Simulator and then rate the quality of motion. This was repeated for 10 motion-base drive algorithms consisting of the nine mentioned above and a no-motion case (NM) in which only buffeting and runway roughness were present. The test matrix is given in Table 2.

The flying sequence consisted of the following items (see Fig. 3), selected to represent the terminal portion of a typical flight:

1) Heading and altitude hold in turbulence.
2) VOR intercept.
3) Deceleration while tracking a VOR radial.
4) Descent.
5) Sidestep maneuver to capture an ILS.

Table 2 Randomized test sequence

Pilot number	Run number									
	R1	R2	R3	R4	R5	R6	R7	R8	R9	R10
P1	AW2	OC1	CW2	CW3	OC3	AW1	AW3	CW1	OC2	NM
P2	CW1	AW3	OC1	OC3	AW1	OC2	NM	CW3	CW2	AW2
P3	CW3	NM	AW3	OC1	OC2	AW2	AW1	CW2	CW1	OC3
P4	AW1	CW1	CW3	OC2	NM	OC3	AW2	AW3	OC1	CW2
P5	OC1	AW1	AW2	CW1	CW2	AW3	CW3	OC3	NM	OC2
P6	OC3	OC2	NM	AW2	OC1	CW1	CW2	AW1	AW3	CW3
P7	AW3	OC3	CW1	NM	AW2	CW2	OC2	OC1	CW3	AW1

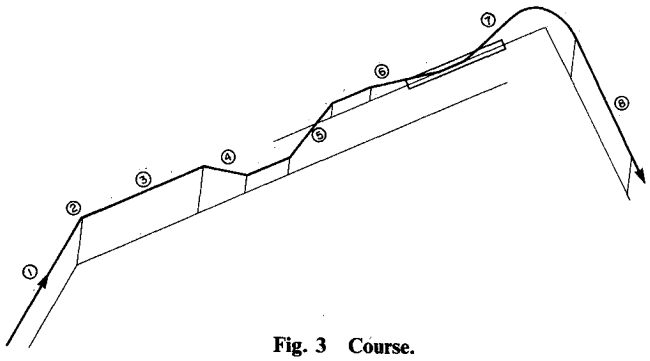

Fig. 3 Course.

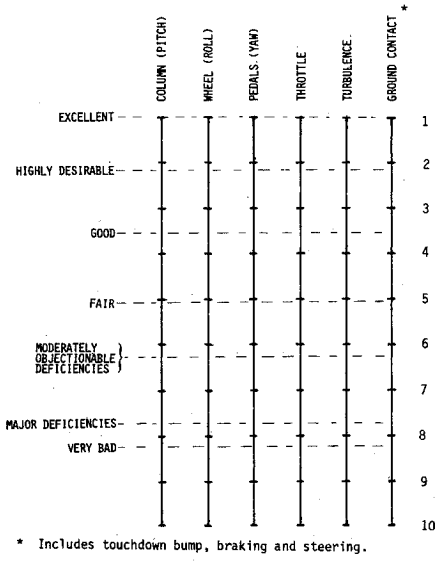

Fig 4 UTIAS rating scale.

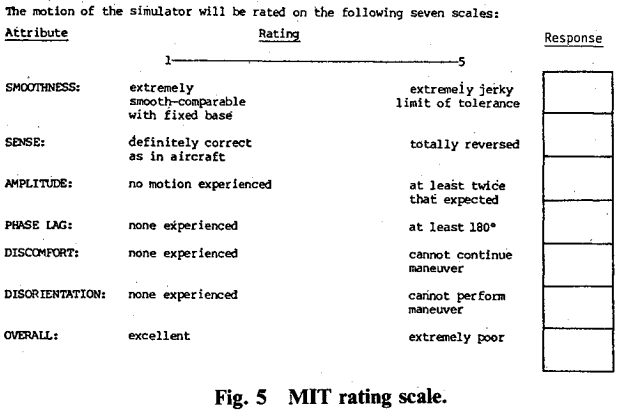

Fig. 5 MIT rating scale.

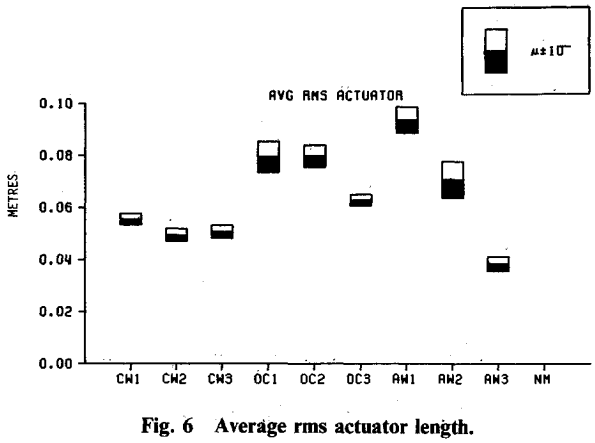

Fig. 6 Average rms actuator length.

Table 3 Pilot experience

Subject number	Current position	Total flying hours	Transport flying hours	Flight simulator hours
1	Captain, DC9	11,000	5,500	500
2	Captain, DC9	14,300	11,400	350
3	F/O, DC9[a]	10,000	5,000	200
4	F/O, L1011	5,000	4,000	250
5	F/O, DC9	5,000	150	250
6	F/O, DC9	5,000	4,000	150
7	S/O, B727[b]	5,500	350	180

[a]F/O–First officer. [b]S/O–Second officer.

6) ILS approach to touchdown.
7) Takeoff and climb-out, including an engine failure.
8) Wheel and rudder induced transients.

Table 3 summarizes the pilots flying and simulator experience. Although we were not able to recruit Boeing 747 pilots, it was believed that with sufficient training useful results would be produced. It was emphasized to the pilots that they were only to judge the quality of the motion cues and not any other aspects of the simulation. It was also made clear to them that they should rate the simulator motion relative to that which would be experienced in an actual aircraft and not relative to that experienced in their airline flight simulators.

Both subjective and objective measurements were used to determine the impact of the motion-base drive algorithms on the pilots. The subjective measurements consisted of two rating scales contained in Figs. 4 and 5. These rating scales are intended to generate information on simulation motion quality in a manner similar to that generated on aircraft handling qualities by the Cooper-Harper rating scale. In addition, the pilots were encouraged to add any comments they wished. The rating scale of Fig. 4 was developed at UTIAS. It is based on work reported in Ref. 22 and the adjectives appearing on the scale are spaced so as to produce an equal interval scale. Immediately following each trial, the pilots were asked to mark on each vertical line their assessment of the quality of motion associated with their control inputs on the column, wheel, rudder pedals and throttle, and also that produced by the turbulence inputs and ground contact. The rating scale of Fig. 5 was developed at the Massachusetts Institute of Technology and is reported in Ref. 7. Using this scale, the pilot must give a numerical rating. The objective measurements covered the pilot's control activity, the performance of the flying tasks and the motion of the flight simulator.

Training took place with the simulator motion base completely shut down (i.e., no buffet or runway roughness present). The pilots were allowed to practice the flying sequence until they felt proficient in the assigned tasks. Typically, 2 h of flying were logged during training in a single session. Next, the evaluation trials were carried out. The 10 motion-base drive algorithms were assigned to each of the seven pilots in a randomized order. Only one morning or afternoon session per day per pilot was allowed. Five flights were performed in a single session by each pilot, requiring two sessions per pilot. Each session lasted approximately 2.5 h.

Results, Analysis, and Discussion

Simulator Motion

As expected, the simulator motion can be strongly influenced by the motion-base drive algorithm. In the present case, an analysis of variance indicated that there was a significant (0.1%) effect on average x and z specific force and rms actuator length (see Fig. 6), and on all the standard deviations of specific force f and angular velocity ω (data analyzed with NM deleted).

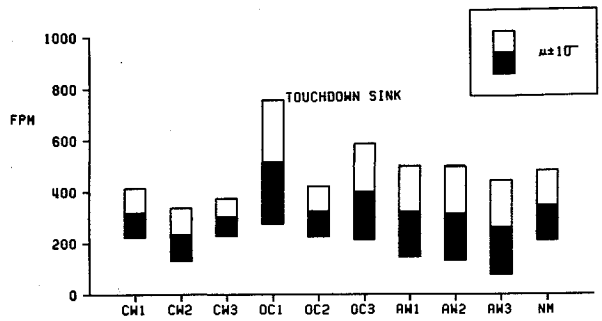

Fig. 7 Touchdown rate of descent.

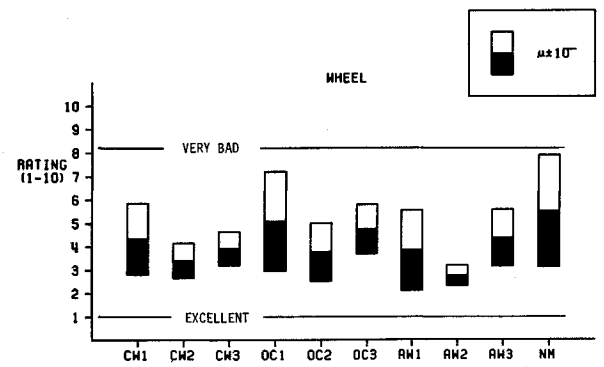

Fig. 8 Pilot ratings of response to wheel inputs (UTIAS).

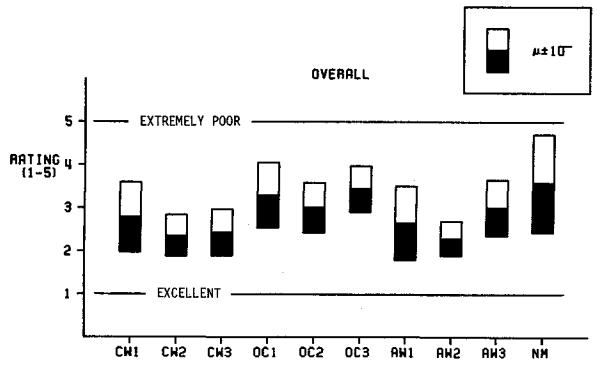

Fig. 9 Overall pilot ratings (MIT).

Pilot's Control Activity and Performance

In general, it was found that there was no influence of motion-drive algorithm type on the pilot's control activity and performance. The greatest variation in performance was noted in the touchdown rate of descent (e.g., see Fig. 7).

Pilot Ratings

In spite of the lack of influence of the motion-base algorithms on such measures as control activity and task performance, there was a definite strong impact on pilot opinion. This was reflected in pilot comments (fully documented in Ref. 9) and pilot ratings.

Figure 8 shows the summary of pilot ratings of simulator response to wheel inputs using the UTIAS scale. Figure 9 does the same for the "overall" rating item included on the MIT scale. It can be seen that the mean values of the ratings (averaged over seven pilots) are affected by the motion-base drive algorithm form.

An analysis of variance was performed on the results from each rating scale. Table 4 shows the results for the UTIAS scale; the MIT scale produced similar values. It is seen that treatment (algorithm) effects are highly significant. In order to highlight the individual items contained in both rating scales, an analysis of variance was performed on subsets of data corresponding to each item in isolation. The results are summarized in Tables 5 and 6 as the probability corresponding to the computed F ratio. It is interesting to note that a repeat of this analysis with the NM data deleted produced essentially the same results.

Table 4 Analysis of variance for the complete set of results using the UTIAS rating scale

Effect[a]	Degrees of freedom	Sum of squares	F value	$P(x > F)$
Subjects	6	44.9026	6.9634	< 0.0001
Treatments	9	220.1021	2.7553	< 0.0001
Subjects × Treatments	54	213.6717	3.6817	< 0.0001
Variables	5	34.8173	6.4793	< 0.0001
Subjects × Variables	30	45.5486	1.4127	0.0810
Treatments × Variables	45	81.3420	1.6819	0.0067
Residual	270	290.1770		
Total	419	930.5613		

[a]"Treatments" refers to the 10 motion-base drive algorithms under study. "Variables" refers to the 6 separate areas that are rated by the pilots.

Table 5 Analysis of variance summary for the UTIAS rating scale $P(x > F)$, %

Subject effects	
Column	87.4
Wheel	97.7
Pedals	13.6
Throttle	0.8
Turbulence	1.3
Ground contact	1.0
Treatment effects[a]	
Column	0.2
Wheel	5.2
Pedals	29.7
Throttle	6.6
Turbulence	<0.1
Ground contact	<0.1

[a]Motion-base drive algorithm

Table 6 Analysis of variance summary for the MIT rating scale $P(x > F)$, %

Subject effects	
Smoothness	6.4
Sense	<0.1
Amplitude	<0.1
Phase lag	<0.1
Discomfort	<0.1
Disorientation	<0.1
Overall	46.5
Treatment effects[a]	
Smoothness	<0.1
Sense	0.6
Amplitude	<0.1
Phase lag	4.1
Discomfort	26.9
Disorientation	16.1
Overall	0.7

[a]Motion-base drive algorithm.

In order of decreasing significance, it was found for the UTIAS scale that the motion-base drive algorithm type affects pilot ratings of ground contact, turbulence, column, wheel, and throttle, with little impact on pedals. For the MIT scale the corresponding sequence was smoothness, amplitude, sense, overall, and phase lag, with little impact on disorientation and discomfort.

The reasons for the particular ratings given the various algorithms are complex. Use must be made of both the recorded pilot comments and the time histories of the individual flights in order to determine their origin. This is done to some degree in Ref. 9.

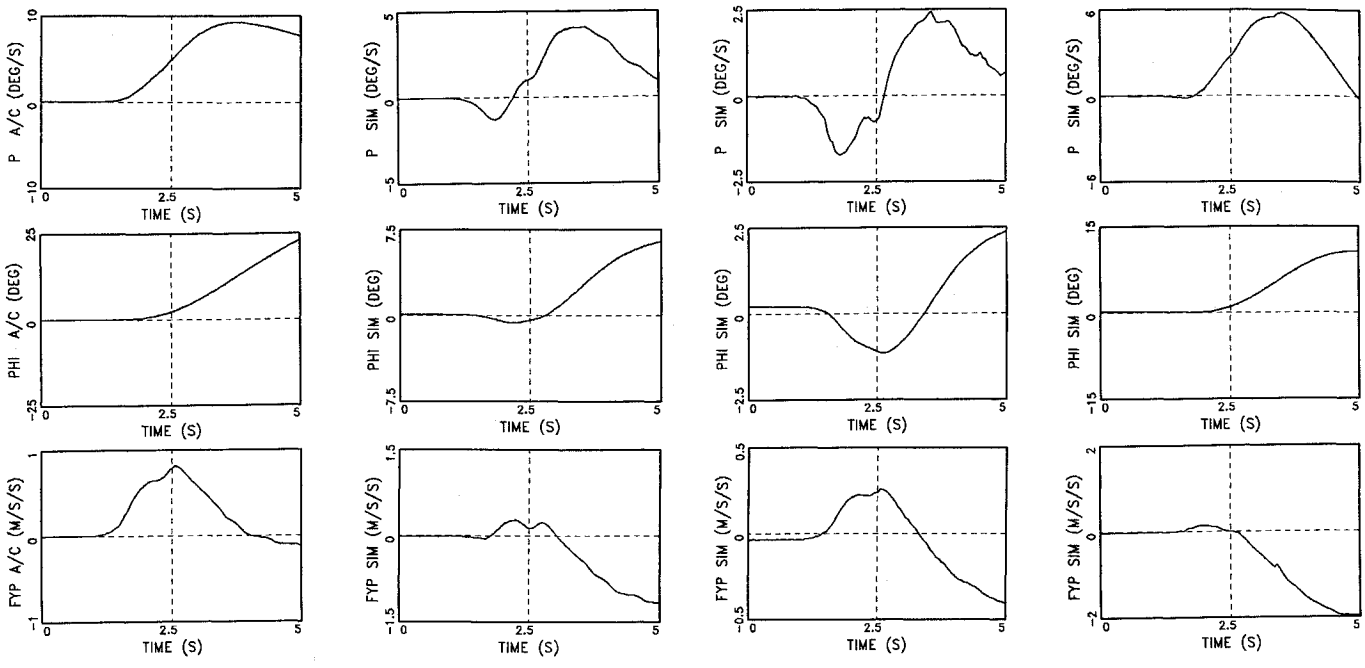

a) Aircraft b) Simulator CW1 c) Simulator OC1 d) Simulator AW1

Fig. 10 Turn entry maneuver.

Table 7 Summary of average pilot ratings (best → worst)

UTIAS rating attributes										
Column	AW2	CW1	CW2	AW1	OC2	CW3	AW3	OC3	OC1	NM
Wheel	AW2	CW2	OC2	AW1	CW3	CW1	AW3	OC3	OC1	NM
Pedals	CW2	AW2	CW1	*AW1*[a]	*CW3*	OC3	OC2	OC1	AW3	NM
Throttle	AW2	CW1	CW2	*AW1*	*OC2*	OC3	OC1	AW3	CW3	NM
Turbulence	AW2	CW2	AW1	CW3	CW1	AW3	OC2	OC1	NM	OC3
Ground contact	AW1	CW1	AW2	CW3	OC1	CW2	OC3	OC2	AW3	NM
MIT rating attributes										
Smoothness	NM	AW3	CW3	AW2	OC2	CW2	AW1	CW1	OC1	OC3
Sense	AW2	CW3	*CW2*	*OC2*	*AW3*	NM	CW1	*OC1*	*OC3*	*AW1*
Amplitude[b]	OC3	AW1	CW1	OC1	CW2	OC2	AW2	CW3	AW3	NM
Phase lag	AW2	CW3	*CW2*	*OC2*	*NM*	AW3	CW1	OC3	AW1	OC1
Discomfort	*AW2*	*AW3*	*CW2*	*CW3*	*OC2*	NM	*OC1*	*AW1*	CW1	OC3
Disorientation	*CW1*	*CW2*	*AW2*	*AW3*	*CW3*	*OC2*	*OC3*	*AW1*	NM	OC1
Overall	AW2	CW2	CW3	AW1	CW1	*AW3*	*OC2*	OC1	OC3	NM

[a]Italics joins identical averages. [b]Most → least.

For example, consider the time histories depicted in Fig. 10. The traces of Figs. 10a and 10b were produced by one pilot carrying out a turn entry (with CW1 in use). Figures 10c and 10d were generated by processing the recorded aircraft response (corresponding to Fig. 10a) through the OC1 and AW1 algorithms. Thus, Figs. 10b–10d show the response of the simulator to the same aircraft motion inputs. In these plots the parameters represent the following: A/C, aircraft; SIM, simulator; FYP, lateral specific force at the pilot's head; PHI, bank angle; and P, roll rate.

The plots of P indicate the presence of an unwanted initial negative peak in the CW1 and OC1 simulator response not found in the aircraft nor in the AW1 roll time histories. The false cue generated by this negative peak was detected by the pilots and led to adverse comments and ratings.

Table 7 summarizes the rank order of the ratings based on the average results. As you read across any row, the algorithms are ordered from best to worst as determined by the mean values of the pilot ratings for the particular attribute listed in the left-hand column. Cases with identical mean ratings are joined together by underlining them. It can be seen that the sequences are somewhat variable across the rated attributes. Despite this it is possible to see some trends.

1) NM appears most often toward the extreme right-hand side of the array, indicating that the no-motion algorithm is not very well liked. (The smoothness case, where NM is ranked first, is not relevant.)

2) AW2 appears most often toward the extreme left-hand side of the array, indicating that it produced the best motion quality in most cases. This is borne out by its ranking as number one under the attribute "overall." (The amplitude case where AW2 is ranked toward the right is only an indication of the amount of motion perceived. From Fig. 5 it is seen that its average value of 2.6 was near 3.0, which indicates a reasonable amount of motion).

3) In the "overall" attribute rating, CW2 is ranked second to AW2. This is consistent with the performance of CW2 in the other categories.

4) The best of the optimal controller algorithms is OC2. Its performance is found to be, on average, slightly to the right of

Table 8 Rating sequences from paired comparison tests

Pilot	Possible sequences (best → worst)		
	Segment 1	Segment 2	Segment 3
1	NM-AW2-CW2-OC2	CW2-AW2-NM-OC2	AW2-NM-0C2-CW2
2	NM-AW2-OC2-CW2	OC2-AW2-CW2-NM	OC2-NM-AW2-CW2
3	CW2-AW2-OC2-NM	CW2-AW2-NM-OC2	NM-AW2-OC2-CW2
4	CW2-AW2-OC2-NM	CW2-AW2-OC2-NM OC2-CW2-AW2-NM AW2-OC2-CW2-NM	AW2-CW2-OC2-NM
5	CW2-OC2-AW2-NM	CW2-OC2-AW2-NM OC2-AW2-CW2-NM AW2-CW2-OC2-NM	CW2-AW2-OC2-NM
6	CW2-AW2-OC2-NM OC2-CW2-AW2-NM AW2-OC2-CW2-NM	AW2-OC2-CW2-NM	OC2-CW2-AW2-NM

center in Table 7. However, OC2 was ranked lower than CW2 and AW2 in almost every category.

5) From the "overall" attribute rating it is seen that all the optimal controller algorithms are ranked below all the classical and adaptive algorithms. The classical and adaptive rankings are intermixed.

Pilot Consistency

The consistency of the pilots in assigning subjective ratings is always a concern. Some idea of this for the present group of pilots can be obtained from the standard deviations of the data plotted in Figs. 8 and 9. A series of tests reported in Ref. 9 and involving the same group of pilots immediately following the tests reported herein (pilots 1–6 in Table 3) can be used to shed further light on their consistency. In these paired comparison tests, three short flight segments were used, each taking 4 min of flying time. Segment 1 involved deceleration and descent (items 3 and 4 of Fig. 3); segment 2 involved an ILS approach and takeoff (items 6 and 7 of Fig. 3, but without the engine failure); segment 3 involved test maneuvers (item 8 of Fig. 3, plus an engine failure). Each of the three segments was studied in a block of experimental trials. A single trial consisted of flying the particular segment twice in close succession but with different motion-base drive algorithms in place. After flying each pair the pilot was asked to indicate which algorithm generated the better motion quality. The motion algorithm cases tested were CW2, OC2, AW2, and NM. All possible pairs were presented to each pilot, using a randomized Latin-Square design.

Based on the results of these tests, the rank orders produced by each pilot are presented in Table 8. In three cases, a pilot was inconsistent in ordering one pair of trials out of the six pairs employed and this resulted in three equally probable rank orderings for that flight segment. In 15 out of 18 cases, the pilots were internally consistent with each of their six paired rankings, agreeing completely with the displayed sequence. However, they displayed a wide range of preferences, depending upon the flight segment. The between-pilot variation can be quantified by using the coefficient of concordance W, defined in Ref. 23, which goes from 1 to 0 as the interpilot consistency goes from perfect agreement to a total lack of agreement. In the present case, values of $W = 0.144$, 0.211, and 0.189 for segments 1–3, respectively, indicate very poor agreement among pilots.

Based on our sample of the airline pilot population, it appears that in rating motion the following is true:

1) Pilots are very self-consistent.

2) Pilots may prefer different motion algorithm properties when carrying out different maneuvers.

3) Interpilot differences are quite large.

Conclusions and Recommendations

1) In the present study, the motion-base drive algorithms had almost no impact on flying performance and control activity.

2) The pilots preferred physical motion to be present in the simulator. They felt that it added to the realism of the simulation and was helpful in the piloting task.

3) In general, each pilot was fairly consistent in his ratings of the various motion-base drive algorithms.

4) There was considerable variability among pilots in the rating process. This was demonstrated by the pilot comments and the small values found for the coefficient of concordance (W) in the paired comparison test analysis.

5) In spite of the variability reported in 4) above, the trends in pilot ratings caused by the different motion-base drive algorithms were significant in the cases of the attributes column, wheel, throttle, turbulence, ground contact, smoothness, sense, amplitude, phase lag and overall. There were no significant trends noted for rudder pedals, discomfort, and disorientation.

6) Under the attribute overall, the pilots ranked the motion-base drive algorithms from best to worst as follows: AW2, CW2, CW3, AW1, CW1, AW3, OC2, OC1, OC3, and NM. However, the other pilot rating responses indicated that the algorithm sequence for any one of the rated attributes might differ from this in detail.

7) No instances of simulator sickness were observed, although there were several complaints of disorientation in the no-motion (NM) runs.

8) Based on the good performance of the coordinated adaptive washout algorithm, it appears worthwhile to investigate its further improvement through a systematic study of alternate forms for its cost function. Also more sophisticated cost functions should be used to give the algorithm more "intelligence" to handle specific situations.

9) Motion-base drive algorithms should be selected to suit the particular simulator, the individual maneuver, the individual degree-of-freedom, and the individual pilot. A means of dynamically achieving this goal should be developed and tested.

Acknowledgments

The work reported in this paper was performed during the final year of a three-year contract held with the Canadian Transportation Development Centre (Contract OSD83-00101, Project 6069). The authors would like to thank all the evaluation pilots who took part in the project. They were unpaid volunteers whose participation was an expression of their professional interest in improving flight simulators. Without their dedicated efforts this study could not have been completed. In addition, we would like to thank the staff of Air Canada and the Canadian Airline Pilots Association who helped us with the fine-tuning of the simulator and the recruitment of the evaluation pilots. The development of the simulator employed in this study was funded by the Canadian Natural Sciences and Engineering Research Council and the Ontario Government.

References

[1]Hosman, R. J. A. W., van der Vaart, J. C., and van de Moesdijk, G. A. J., "Optimization and Evaluation of Linear Motion Filters," Dept. of Aerospace Engineering, Delft University of Technology, the Netherlands, Memo M-326, March 1979.

[2]Irish, P. A. and Brown, J. E., "Subjective Motion Discrimination in the Simulator for Air-to-Air Combat," AFHRL-TR-78-26, Aug. 1978.

[3]Hofmann, L. G. and Riedel, S. A., "Manned Engineering Flight Simulation Validation, Part I: Simulation Requirements and Simulator Motion System Performance," AFFDL-TR-78-192, Part 1, Feb. 1979.

[4]Parrish, R. V. and Martin, D. J., Jr., "Application of Nonlinear Adaptive Motion Washout to Transport Ground-Handling Simulation," NASA TM 84568, Feb. 1983.

[5]Parrish, R. V. and Martin, D. J., Jr., "Comparison of a Linear and a Nonlinear Washout for Motion Simulators Utilizing Objective and Subjective Data from CTOL Transport Landing Approaches," NASA TN D-8157, June 1976.

[6]Bitner, M. E., "Investigation of Motion Base Drive Techniques," NADC-77306-20, March 1978.

[7]Bussolari, S. R., Sullivan, R. B., and Young, L. R., "Vestibular Models for Design and Evaluation of Flight Simulator Motion," presented at the Royal Aeronautical Society Conference on Advances in Flight Simulation Visual and Motion Systems, London, April 1986.

[8]Grant, P. R., "Motion Characteristics of the UTIAS Flight Research Simulator Motion-Base," University of Toronto, Canada, UTIAS TN 261, July 1986.

[9]Reid, L. D. and Nahon, M. A., "Flight Simulation Motion-Base Drive Algorithms: Part 3–Pilot Evaluations," University of Toronto, Canada, UTIAS Rept. 319, Dec. 1986.

[10]Leung, Y. M., "Solution of the General Flight Equations in Real Time," M.A.Sc. Thesis, UTIAS, University of Toronto, Canada, 1985.

[11]Hanke, C. R. and Nordwall, D. R., "The Simulation of a Jumbo Jet Transport Aircraft, Volume 11: Modeling Data," NASA CR-114494, Sept. 1970.

[12]Hanke, C. R., "The Simulation of a Large Jet Transport Aircraft, Volume 1: Mathematical Model," NASA CR-1756, March 1971.

[13]Gerlach, O. H. and Baarspul, M., "Calculation of the Response of an Aircraft to Random Atmospheric Turbulence, Part 11: Asymmetric Motions," Dept. of Aeronautical Engineering, Delft, University of Technology, the Netherlands, Rept. VTH-139, April 1968.

[14]van de Moesdijk, G. A. J., "The Description of Patchy Atmospheric Turbulence, Based on a Non-Gaussian Simulation Technique," Dept. of Aeronautical Engineering, Delft University of Technology, the Netherlands, Rept. VTH-192, Feb. 1975.

[15]van de Moesdijk, G. A. J., "Non-Gaussian Structure of the Simulated Turbulent Environment in Piloted Flight Simulation," Dept. of Aerospace Engineering, Delft University of Technology, the Netherlands, Memo M-304, April 1978.

[16]Baarspul, M., "The Generation of Motion Cues on a Six-Degrees-of-Freedom Motion System," Dept. of Aerospace Engineering, Delft University of Technology, the Netherlands, Rept. LR-248, June 1977.

[17]Parrish, R. V., Dieudonne, J. E., and Martin, D. J., Jr., "Motion Software for a Synergistic Six-Degree-of-Freedoms Motion Base," NASA TN D-7350, Dec. 1973.

[18]Schmidt, S. F. and Conrad, B., "Motion Drive Signals for Piloted Flight Simulators," NASA CR-1601, May 1970.

[19]Sivan, R., Ish-Shalom, J., and Huang, J.-K., "An Optimal Control Approach to the Design of Moving Flight Simulators," *IEEE Transactions on Systems, Man, and Cybernetics*, Vol. SMC-12, No. 6, Nov.–Dec. 1982, pp. 818–827.

[20]Reid, L. D. and Nahon, M. A., "Flight Simulation Motion-Base Drive Algorithms: Part 1–Developing and Testing the Equations," University of Toronto, Canada, UTIAS Rept. 296, Dec. 1985.

[21]Reid, L. D. and Nahon, M. A., "Flight Simulation Motion-Base Drive Algorithms: Part 2–Selecting the System Parameters," University of Toronto, Canada, UTIAS Rept. 307, May 1986.

[22]McDonnell, J. D., "An Application of Measurement Methods to Improve the Quantitative Nature of Pilot Rating Scales," *IEEE Transactions on Man-Machine Systems*, Vol. MMS-10, No. 3, Sept. 1969, pp. 81–92.

[23]Seaver, D. A. and Stillwell, W. G., "Procedures for Using Expert Judgment to Estimate Human Error Probabilities in Nuclear Power Plant Operations," U.S. Nuclear Regulatory Commission, NUREG CR-2743, 1983, pp. A-1–A-12.